1st International Conference on Sensing Technology
November 21-23, 2005 Palmerston North, New Zealand

Application of Optical Fiber Sensor for the Tactile Sensor System

Jin-Seok Heo, Jong-Ha Chung, and Jung-Ju Lee*
Korea Advanced Institute of Science and Technology ,
Daejeon, Republic of Korea
leejungju@kaist.ac.kr*

Abstract

This paper describes 3x3 force sensor arrays using fiber Bragg gratings (FBG) and transducers for tactile sensation to detect a distributed normal force. The transducer is designed such that it is not affected by chirping and light loss. We also present the fabrication process and experimental verification of the prototype sensors. Experimental tests show that the newly designed sensors have good performance: good sensitivity, repeatability, and no-hysteresis. The load calibration is accomplished by a verified uniaxial load cell. In order to provide a more precise measurement, temperature compensation is applied to all taxels. These force sensor arrays are flexible enough to be attached to a curved surface and they also have simple wiring compared with other types of small force sensors for tactile sensation.

Keywords: fiber Bragg grating sensor, tactile sensor array, taxel

1 Introduction

Sensory information of human skin for feeling materials and determining many of their physical properties is provided by sensors in the skin. This tactile information is related to the sense of touch, one of the five senses including sight, hearing, smell, and taste. Presently, many researchers are attempting to apply the five senses to intelligent robot systems. In particular, many kinds of tactile sensors combining small force sensors have been introduced for intelligent robots, teleoperational manipulators, and haptic interfaces. These tactile sensors, which are capable of detecting contact force, vibration, texture, and temperature, can be recognized as the next generation information collection system. Future applications of engineered tactile sensors include robotics in medicine for minimally invasive and micro surgeries, military uses for dangerous and delicate tasks, and automation of industry.

Some tactile sensors and small force sensors using microelectromechanical systems (MEMS) technology have been introduced. MEMS tactile sensing work has mainly focused on silicon-based sensors that use piezoresistive [1, 2] or capacitive sensing [3, 4]. These sensors have been realized with bulk and surface micromachining methods. Polymer-based devices that use piezoelectric polymer films [5, 6] such as polyvinylidene fluoride (PVDF) for sensing have also been demonstrated.

Although these sensors offer good spatial resolution owing to the use of MEMS techniques, there remain some problems with respect to application to practical systems. In particular, devices that incorporate brittle sensing elements such as silicone based diaphragms or piezoresistors, including even those embedded in protective polymers, have not proven to be a reliable interface between a robotic manipulator and the manipulated object. Previous efforts have been hindered by rigid substrates, fragile sensing elements, and complex wiring. These drawbacks can be compensated for by utilizing flexible optical fiber sensors and transducers. In addition, optical fiber sensors have immunity to electro magnetic fields and can be easily multiplexed. Therefore, in this paper, we present a newly designed optical fiber force sensor and 3x3 sensor arrays, which are the first step toward realizing a tactile sensor using optical fiber sensors (FBG).

2 Design of Flexible Sensor

2.1 Principle of FBG

FBG sensors based on wavelength-division multiplexing (WDM) technology are ideally suited for distributed strain monitoring. FBG sensors are easily multiplexed and offer many advantages such as linear response and relative measurement. The basic principle of an FBG-based sensor system lies in the monitoring of the wavelength shift of the returned Bragg-signal,as a function of the measurand (e.g. strain, temperature, and force). The Bragg wavelength is related to the refractive index of the material and the grating pitch. Sensor systems involving such gratings typically work by injecting light from a spectrally broadband source into the fiber, with the result that the grating reflects a narrow spectral

component at the Bragg wavelength, or in transmission this component is missing from the observed spectrum. Fig.1 illustrates this process simply and schematically.

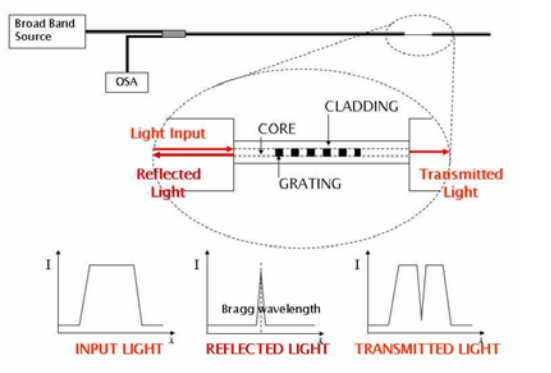

Figure 1 Fiber Bragg Grating sensor encoding operation

The intensity of the reflected optical signal is a function of the Bragg grating wavelength, which is related to the applied strain on the FBG. Therefore, the dynamic strain can be derived from the intensity change measurement as a function of the wavelength of the reflected optical signal. The operation of an FBG is based on a periodic, refractive index change that is produced in the core of an optical fiber by exposure to an intense UV interference pattern. This grating structure results in the reflection of the light at a specific narrow band wavelength, called the Bragg wavelength. The Bragg condition is given by

$$\lambda_B = 2n_e\Lambda \qquad (1)$$

where λ_B is the Bragg wavelength of the FBG, n_e is the effective index of the fiber core, and Λ is the grating period. The Bragg wavelength shift due to strain and temperature can be expressed as

$$\Delta\lambda_B = \lambda_B\left[\left(\alpha_f + \xi_f\right)\Delta T + \left(1 - p_e\right)\Delta\varepsilon\right] \qquad (2)$$

$$p_e = \left(\frac{n^2}{2}\right)\left[p_{12} - \nu\left(p_{11} - p_{12}\right)\right] \qquad (3)$$

where α_f is the coefficient of the thermal expansion (CTE), ξ_f is the thermo-optical coefficient, and p_e is the strain-optical coefficient of the optical fiber. The value of p_e =0.227 [7] was measured experimentally and used for this study. If there is no temperature change, we can measure the strain from the wavelength shift as

$$\varepsilon = \frac{1}{\left(1 - p_e\right)}\frac{\Delta\lambda_B}{\lambda_B} \qquad (4)$$

2.2 Design of Transducer using FEM

First, there are two major factors that must be considered upon designing the transducer of FBG force sensors. The first is light loss by micro bending, as shown in Figure 2. If micro bending occurs in the optical fiber, the intensity of the reflected light is remarkably decreased, and as a result the proper Bragg wavelength cannot be measured. As micro bending often occurs in a small size sensor, the transducer must be designed to minimize this effect.

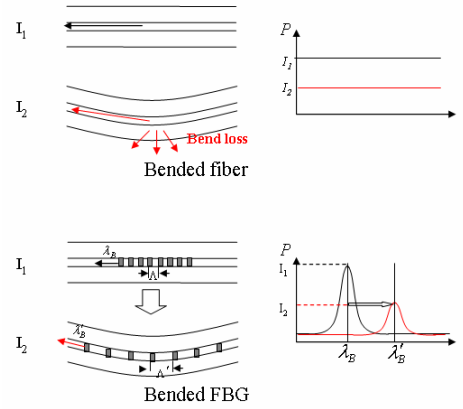

Figure 2 Micro bending effect of Bragg wavelength

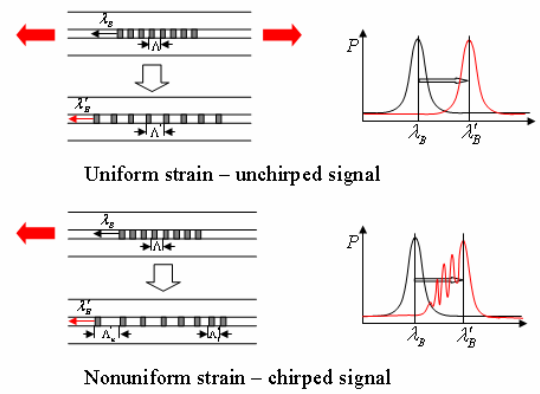

Figure 3 Chirping effect of FBG

The FBG force sensor uses a diaphragm type transducer, which can be easily deformed by an external force, as shown in Figure 4. This transducer consists of a contact mesa and membrane. When the external force concentrates on the contact mesa, the membrane is deflected. As the FBG sensor is embedded in the membrane, the deflection of the membrane induces elongation of the FBG. As note above, the Bragg wavelength can be changed by this elongation of the FBG sensor. Therefore, we can determine the external force change by measuring the Bragg wavelength shift. The transducer is made of PDMS (Polydimethylsiloxane), a kind of flexible silicone rubber.

First, the capacity of the flexible force sensor must be determined. As this sensor will be applied to a tactile sensor system, a maximum force range of 5N, which is similar to the capacity of human skin, is established.

The length of the FBG used in this sensor is 10mm. As the length of the FBG is reduced, a correspondingly smaller force sensor can be realized. Some studies utilizing extremely short length (dozens of μm) FBGs [8] have been introduced. If such a short can be applied to this flexible force sensor, the size of the sensor can be accordingly minimized. The maximum size of the sensor is determined as 20mm, which is similar to the maximum spatial resolution of human skin. Therefore, the diameter of the cavity bottom space under the membrane of the transducer is selected to be 15mm. The thickness of the contact mesa, which does not influence the performance of the force sensor, is 3mm. The thickness of the membrane is 4mm, which is sufficient for the membrane not to be deflected by the weight of the contact mesa.

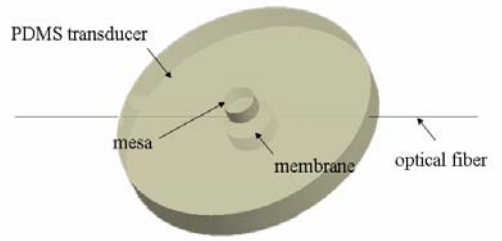

Figure 4 Structure of the flexible force sensor

Next, the position of the FBG must be decided. In the general case of a diaphragm type force sensor, the maximum strain position of the transducer constitutes a suitable embedding position for the sensing element. However, in the present case of using a 10mm FBG sensor, the maximum strain position is very short compared with the length of the FBG. Therefore, 10mm FBG experiences a non-uniform strain distribution over the whole length of the FBG when it is embedded at this short maximum strain position. For this reason, a uniform distributed strain position in a 10mm span must be found so as to avoid a chirping effect. The deformation of the silicone rubber was simulated using a finite element analysis (FEA) to find the uniform distributed strain position.

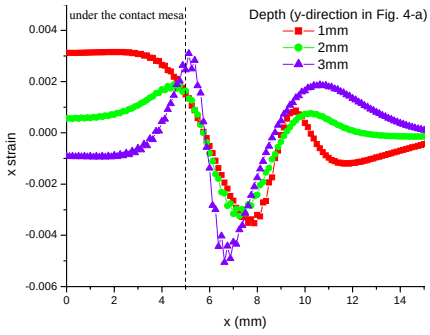

Figure 5 Strain distribution along the x axis

As the structure of the transducer is symmetric, a half geometric model and a 2-dimensional element model were adopted. The optical fiber was excluded from the FEA model, because the single mode optical fiber employed here has a very small diameter (250 μm) compared with the whole size of the transducer. That is, the sensor model has only a silicone rubber model and we assumed that the deformation of the optical fiber follows the deformation of the silicone rubber. As the deformation of the silicone rubber is very small, we used a general elastic solver to verify the deformation. The elastic modulus of PDMS is 9.2MPa and Poission's ratio is 0.49.

The strain distribution of the axial direction of the optical fiber is shown in Figure 5. Although the strain distribution fluctuates somewhat, we can see that the position under the contact mesa of the transducer has a more uniform strain distribution than any other position. In addition, more strain occurs at the deeper position under the contact mesa.

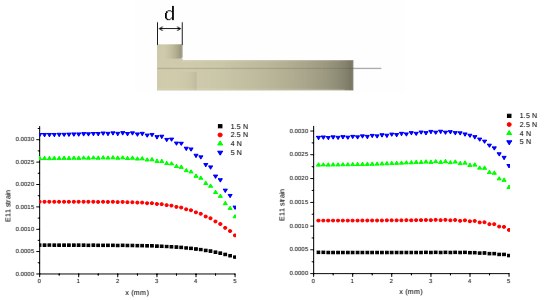

(a) (b)

Figure 6 Strain distribution of different diameters of the contact mesa when (a) d = 4mm, and (b) d = 5mm

Considering the diameter of the single mode optical fiber, 1mm depth is suitable for this transducer in terms of obtaining good sensitivity. As shown in Figure 6, the strain distribution under the contact mesa is calculated for different diameters of contact mesa. The results indicate that a larger contact mesa yields wide uniform strain distribution. Therefore, the diameter of the contact mesa of 10mm, which corresponds with the length of the FBG, is suitable considering the size of the transducer and the length of the FBG. Figure 7 shows the dimensions of the diaphragm type force sensor prototype.

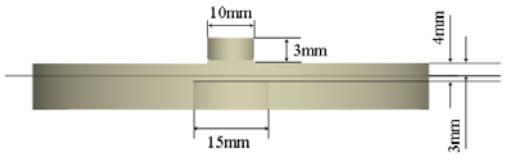

Figure 7 Dimensions of the prototype flexible sensor

Figure 8 shows the experimental verification that the chirping effect is minimized. When the FBG is embedded in the side of the membrane, the Bragg wavelength is distorted, as shown in Figure 8a, in a/as a result of non-uniform strain distribution. However, there is no distortion of Bragg wavelength when the FBG is under the contact mesa of the transducer, as shown in Figure 8b.

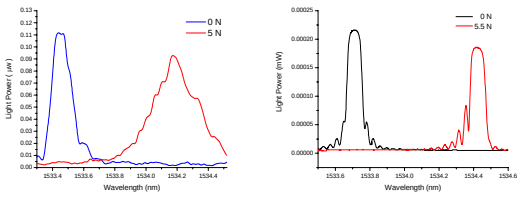

(a) (b)

Figure 8 Experimental verification that chirping is minimized: (a) chirping, (b) minimized chirping

The other factor is chirping, which causes distortion of the Bragg signal. In this case, a non-uniform strain distribution along the whole length of the FBG leads to a distorted Bragg wavelength, known as chirping (Figure 3), which interferes with the determination of the exact Bragg wavelength.

3 Fabrication and Evaluation of Taxel

Figure 9 shows the fabrication process of the diaphragm type force sensor prototype. The first step of the fabrication process is making the molding frame. Once the molding frame is prepared, an FBG is aligned at the center of that the frame. Next, PDMS is poured up to the desired height of the transducer. After pouring and curing the PDMS, the contact mesa, which is also made of PDMS, is attached to the center of membrane. Finally, the molding frame is removed.

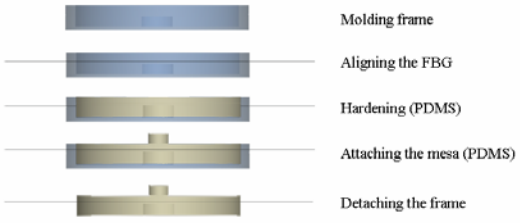

Figure 9 Fabrication process of a taxel

The fabricated prototype sensors were calibrated by the verified uniaxial loadcell, as shown in Figure 10. The broadband light source having 1527~1602nm wavelength is incident to the optical fiber and the isolator plays a role of preventing counterflow of the reflected light to the broadband light source. The light from the isolator is separated by a 2 by 1 coupler. The light that transmits the coupler proceeds to the Bragg grating. The reflected light experiencing the applied load is sent to a tunable Fabry-Perot filter (TFPF), which can detect the Bragg wavelength. The Bragg wavelength shift is observed and plotted via LabVIEW data acquisition program to calculate the applied force. The prototype sensor is set on the z-stage and is aligned to the loadcell. As the z-stage moves up, the contact mesa of the prototype sensor is pressed by the load cell. That is, the detected forces by the loadcell and by the prototype sensor have the same absolute values, but have different directions. Therefore, the prototype force sensor can be directly calibrated by the verified load measured by the uniaxial reference load cell.

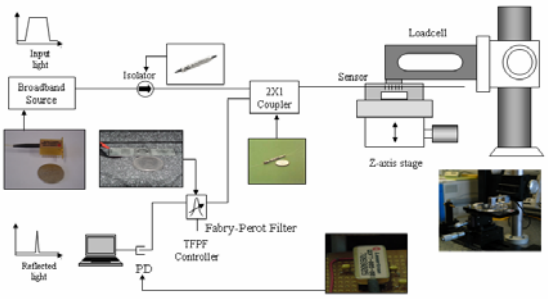

Figure 10 Calibration system of prototype sensor

The change of temperature and strain influences the Bragg wavelength shift of the FBG sensor simultaneously. To measure the exact external force change, the shift of Bragg wavelength by the temperature change must be excluded.

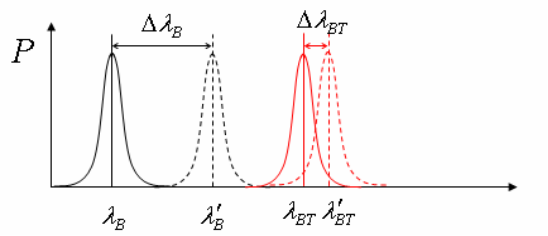

Figure 11 Temperature compensation of flexible force sensor

As shown in Figure 11, a reference FBG sensor must be added for the temperature compensation. This reference FBG sensor, which does not have a diaphragm, detects the Bragg wavelength shift by the temperature change. Therefore, the Bragg wavelength shift by the strain change can be calculated by subtracting the Bragg wavelength shift of the reference fiber from the total Bragg wavelength shift. The temperature compensated Bragg wavelength is given by

$$\begin{aligned} \Delta\lambda_B &= \lambda'_B - \lambda_B \\ \Delta\lambda_{BT} &= \lambda'_{BT} - \lambda_{BT} \\ \Delta\lambda_{TC} &= \Delta\lambda_B - \Delta\lambda_{BT} \end{aligned} \qquad (5)$$

where $\Delta\lambda_B$, $\Delta\lambda_{BT}$, and $\Delta\lambda_{TC}$ describe the Bragg wavelength shift including the strain and temperature effect, the Bragg wavelength shift by the temperature change, and the temperature compensated Bragg wavelength shift, respectively.

The plots of the Bragg wavelength change by the applied force are shown in Figure 12. There is a non-linear relation between the Bragg wavelength change and the applied force in the diaphragm type sensor. This non-linear relation appears to be caused by the non-linear material property of the transducer. This relationship between the Bragg wavelength shift and the applied force is found to be approximately 2nd

order polynomial based on a curve fit of Figure 12. The accuracies of the prototype sensors are 99.9% and the resolutions are about 0.005N. The resolution of these force sensors depends on that of the tunable Fabry-Perot filter that detects the Bragg wavelength (1pm). Namely, if the resolution of the TFPF is improved, that of the force sensor will be enhanced.

We assessed the repeatability and the hysteresis of the prototype sensors. Tests of repeatability were accomplished by 3 iterations of the same loading conditions for the specified prototype force sensors. Tests of hysteresis were accomplished to observe differences between loading and unloading conditions. Figure 13 illustrates that the force sensor displays good repeatability and no hysteresis.

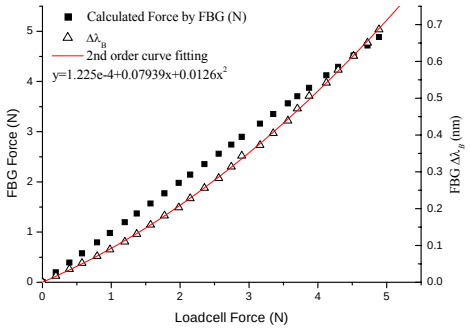

Figure 12 Plots of Bragg wavelength shift and prototype force signal vs. load cell signal

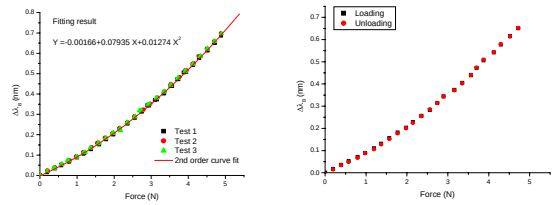

(a) (b)

Figure 13 Experimental verification of the prototype sensor: (a) repeatability of diaphragm type sensor, (b) hysteresis of diaphragm type sensor

4 Fabrication and Evaluation of Array Sensor

We fabricated 3x3 sensor arrays, which are composed of only three optical fibers having 3 FBGs, respectively, and an integrated transducer. The position of each sensor is selected as shown in Figure 14.

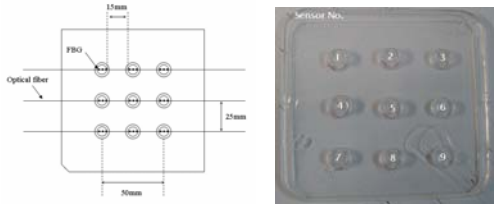

Figure 14 3x3 array sensor

In the case of the diaphragm type sensor array, the distance of each sensor, namely, the spatial resolution, is 25mm, which is similar to the resolution of human back skin.

Table 1. 2nd order polynomial approximation of each sensor (diaphragm type sensor array)

Coefficient / Sensor No.	A	B	C
1	-0.0012	0.0477	0.0026
2	-0.0182	0.0445	0.0030
3	-0.0011	0.0521	0.0035
4	0	0.0210	0.0040
5	0	0.0415	0.0032
6	0.0016	0.0498	0.0035
7	-0.0026	0.0359	0.0039
8	-0.0010	0.0475	0.0034
9	0.0011	0.0446	0.0033

($y=A+Bx+Cx^2$ y: applied force, x: wavelength shift)

9 FBGs, which are embedded in a sensor array, have their own Bragg wavelength. The different Bragg wavelengths make different peak points and these peak points are detected at a photo-diode (PD), as shown in Figure 15. The shifts of each Bragg wavelength are observed and plotted via a LabVIEW data acquisition program to calculate the distributed force. The shifts of each Bragg wavelength are measured by a tunable Fabry-Perot filter, which is under the control of the LabVIEW program. Therefore, the shifts of each Bragg wavelength, which represents the change of distributed force, can be detected simultaneously through this interrogation system using wavelength division multiplexing (WDM). As noted above, the relationship between the Bragg wavelength shift and the applied force of the diaphragm type sensor array is expressed as a 2nd order polynomial function, respectively. The relations of each sensor were verified to determine the distributed force directly using the calibration system, as shown in Figure 10. Table 1 shows the experimentally evaluated coefficients of these approximations.

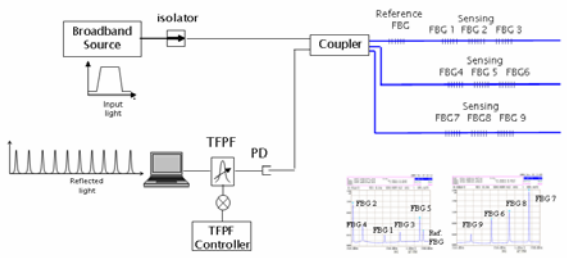

Figure 15 Interrogation system of the 3x3 array sensor

Experiments for verification of the 3x3 sensor arrays were accomplished by applying the distributed force and the point force. Figure 16a shows the graph of 1N on the 5th taxel of the diaphragm type sensor array and Figure 16b shows the graph of 1N distributed on the 5th, 6th, 8th, and 9th taxels of the diaphragm type sensor array. Each taxel displays 0.25N

These experimental results show that the optical fiber force sensor arrays are effective in terms of practical application to a real system and display good performance compared with other kinds of force sensor arrays. However, the proposed sensors are somewhat larger than MEMS-based small sensor arrays and the system requires high cost.

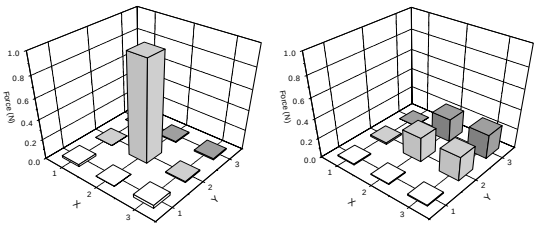

(a) (b)

Figure 16 Evaluation of 3x3 array sensors: (a) 1N on 5th taxel of diaphragm type sensor array, (b) 1N on 5th, 6th, 8th, 9th taxels of diaphragm type sensor array

5 Conclusion

In this paper, force sensor array using a fiber Bragg grating for a tactile sensor were newly designed and experimentally evaluated. In the case of the diaphragm type sensor array, the optimum embedding position of the fiber Bragg grating in terms of minimizing chirping was found using a finite element analysis of the PDMS transducer. This sensor can be easily fabricated via molding and aligning the FBG sensor. There is a non-linear relation between the applied force and the Bragg wavelength shift. The spatial resolution of the sensor array is 25mm and the used length of FBG is 10mm. If a shorter length FBG were used, then a smaller size flexible force sensor could be realized and the spatial resolution would be enhanced. The fabricated prototype sensors displayed good performance, in particular, good repeatability, high accuracy and resolution, and no hysteresis. In order to measure the distributed force more precisely, temperature compensation by adding an additional FBG that does not have a transducer was utilized. In addition, by regarding the shifted Bragg wavelength resulting from the small deformation as the new Bragg wavelength, zero setting was applied to all taxels. The performance of the 3x3 sensor arrays was experimentally verified. The 3x3 sensor arrays have 9 Bragg grating sensors in 3 fibers. That is, 3 Bragg gratings are induced in each fiber. The wavelength division multiplexing method was used in these sensor arrays and they are sufficiently flexible to attach to a curved surface and quantitative measuring as possible in this situation. The proposed sensor arrays exhibited good performance for a first generation sensor design using optical fiber sensors (FBGs). These 3x3 sensor arrays are a major step towards realizing tactile sensor skin using optical fiber sensors, which has many strengths (immunity to electromagnetic field, high resolution, simple wiring, corrosion-resistance, high capacity and speed of data processing, high flexibility) compared with previous efforts. However, there is room for improvement with regard to fabricating cost as well as spatial resolution.

6 Acknowledgements

This research (paper) was performed for the Intelligent Robotics Development Program, one of the 21st Century Frontier R&D Programs funded by the Ministry of Commerce, Industry and Energy of Korea.

7 References

[1] B. J. Kane, M. R. Cutkosaky, T. A. Kovacs, “A traction stress sensor array for use in high resolution robotic tactile image”, *J. Microelectromech. Syst.* 9 (2000) 425-434.

[2] D. J. Beebe, A. S. Hseih, D. D. Denton, R. G. Radwin, “A silicon force sensor for robotics and medicine”, *Sens. Actuat. A* 50 (1995), 55-56

[3] B. L. Gray, R. S. Fearing, “A surface micromachined micro tactile sensor array”, *Proceedings of the IEEE International Conference on Robotics and Automation*, 1996, p1-6

[4] M. Leineweber, G. Pelz, M. Schmoidt, H. Kappert, G. Zimmer, “New tactile sensor chip with silicone rubber cover”, *Sens. Acuat. A* 84 (2000) 236-245

[5] E. S. Kolesar, C. S. Dyson, “Object image with a piezoelectric robotic tactile sensor”, *J. Microelectromech. Syst.* 4 (1995) 87-96

[6] R. R. Reston, E. S. Kolesar, “Robotic tactile sensor array fabricated from a piezoelectric polyvinylidine fluoride film”, *Proceeding of the IEEE NAECON*, 1990, pp1139-1144.

[7] C. Y. Ryu, C. S. Hong, C. G. Kim, S. B. Lee, and S. S. Choi, “Strain measurement of the laminated composite using attached fiber Bragg grating sensor”, *Proceeding of the 3rd optoelectronics and communications conference*, 1998, pp272~273.

[8] Meng-Chou Wu, R. S. Rogowski, and K. K. Tedjojuwono, “Fabrication of extremely short length fiber Bragg grating for sensor application”, *Sensors, Proceeding of IEEE*, vol. 1, 2002, pp 49~55.